



# Extended depth of focus intraocular lens: chromatic performance

MARIA S. MILLÁN\* AND FIDEL VEGA

*Departament d'Òptica i Optometria, Universitat Politècnica de Catalunya, BARCELONATECH  
Violinista Vellsolà 37, 08222 Terrassa, Spain*

\*[m.millan@upc.edu](mailto:m.millan@upc.edu)

**Abstract:** We describe a first-and-second-diffractive-order intraocular lens ((1<sup>st</sup>,2<sup>nd</sup>)DIOL) within the class of hybrid refractive-diffractive designs for intraocular lenses (IOLs) and analyse its properties of focus extension and compensation of longitudinal chromatic aberration (LCA), particularly for lenses with low addition. Power, energy efficiency and their wavelength dependence are extended from monofocal IOL and conventional bifocal zeroth-and-first-diffractive-order IOL ((0<sup>th</sup>,1<sup>st</sup>)DIOL) to (1<sup>st</sup>,2<sup>nd</sup>)DIOL of low addition. Compensation of LCA is experimentally assessed in optical bench through the through-focus energy efficiency of three Tecnis IOLs with red, green and blue illuminations: ZA9003 (monofocal), ZKB00 (bifocal (0<sup>th</sup>,1<sup>st</sup>)DIOL with + 2.75 D add) and Symphony ZXR00. We prove Tecnis Symphony ZXR00 IOL can be considered an example of (1<sup>st</sup>,2<sup>nd</sup>)DIOL design of low addition, with LCA compensation in both the distance and intermediate foci, whereas the bifocal (0<sup>th</sup>,1<sup>st</sup>)DIOL does not compensate in the distance focus. However, the energy efficiency of (1<sup>st</sup>,2<sup>nd</sup>)DIOL for wavelengths other than the design wavelength is markedly more asymmetric.

© 2017 Optical Society of America

**OCIS codes:** (260.0260) Physical optics; (330.7335) Visual optics, refractive surgery; (170.4460) Ophthalmic optics and devices; (050.1965) Diffractive lenses; (220.0220) Optical design and fabrication; (220.1010) Aberrations (global); (220.1000) Aberration compensation; (120.3620) Lens system design; (120.4800) Optical standards and testing; (120.4820) Optical systems.

## References and links

1. A. L. Cohen, "Practical design of a bifocal hologram contact lens or intraocular lens," *Appl. Opt.* **31**(19), 3750–3754 (1992).
2. A. L. Cohen, "Diffractive bifocal lens designs," *Optom. Vis. Sci.* **70**(6), 461–468 (1993).
3. J. A. Davison and M. J. Simpson, "History and development of the apodized diffractive intraocular lens," *J. Cataract Refract. Surg.* **32**(5), 849–858 (2006).
4. F. Vega, F. Alba-Bueno, and M. S. Millán, "Energy distribution between distance and near images in apodized diffractive multifocal intraocular lenses," *Invest. Ophthalmol. Vis. Sci.* **52**(8), 5695–5701 (2011).
5. S. Ravikumar, A. Bradley, and L. N. Thibos, "Chromatic aberration and polychromatic image quality with diffractive multifocal intraocular lenses," *J. Cataract Refract. Surg.* **40**(7), 1192–1204 (2014).
6. J. F. Alfonso, L. Fernández-Vega, M. B. Baamonde, and R. Montés-Micó, "Prospective visual evaluation of apodized diffractive intraocular lenses," *J. Cataract Refract. Surg.* **33**(7), 1235–1243 (2007).
7. A. Alarcon, C. Canovas, R. Rosen, H. Weeber, L. Tsai, K. Hileman, and P. Piers, "Preclinical metrics to predict through-focus visual acuity for pseudophakic patients," *Biomed. Opt. Express* **7**(5), 1877–1888 (2016).
8. G. Cardona, F. Vega, M. A. Gil, C. Varón, J. A. Buil, and M. S. Millán, "Visual acuity and image quality in 5 diffractive intraocular lenses," *Eur J Ophthalmol.* Jun 26:0 [Epub ahead of print] (2017).
9. N. López-Gil and R. Montés-Micó, "New intraocular lens for achromatizing the human eye," *J. Cataract Refract. Surg.* **33**(7), 1296–1302 (2007).
10. H. A. Weeber and P. A. Piers, "Theoretical performance of intraocular lenses correcting both spherical and chromatic aberration," *J. Refract. Surg.* **28**(1), 48–52 (2012).
11. M. Vinas, C. Dorronsoro, D. Cortes, D. Pascual, and S. Marcos, "Longitudinal chromatic aberration of the human eye in the visible and near infrared from wavefront sensing, double-pass and psychophysics," *Biomed. Opt. Express* **6**(3), 948–962 (2015).
12. M. S. Millán, F. Vega, and I. Ríos-López, "Polychromatic image performance of diffractive bifocal intraocular lenses: longitudinal chromatic aberration and energy efficiency," *Invest. Ophthalmol. Vis. Sci.* **57**(4), 2021–2028 (2016).
13. D. Faklis and G. M. Morris, "Spectral properties of multiorder diffractive lenses," *Appl. Opt.* **34**(14), 2462–2468 (1995).

14. D. W. Sweeney and G. E. Sommargren, "Harmonic diffractive lenses," *Appl. Opt.* **34**(14), 2469–2475 (1995).
15. V. Calero, P. García-Martínez, J. Albero, M. M. Sánchez-López, and I. Moreno, "Liquid crystal spatial light modulator with very large phase modulation operating in high harmonic orders," *Opt. Lett.* **38**(22), 4663–4666 (2013).
16. J. Albero, P. García-Martínez, J. L. Martínez, and I. Moreno, "Second order diffractive optical elements in a spatial light modulator with large phase dynamic range," *Opt. Lasers Eng.* **51**(2), 111–115 (2013).
17. H. A. Weeber, "Multi-ring lens, systems and methods for extended depth of focus," US Patent No. 2014/0168602 A1. Pub. Date: Jun 19, 2014.
18. D. Gatinel and J. Loicq, "Clinically Relevant Optical Properties of Bifocal, Trifocal, and Extended Depth of Focus Intraocular Lenses," *J. Refract. Surg.* **32**(4), 273–280 (2016).
19. J. J. Esteve-Taboada, A. Domínguez-Vicent, A. J. Del Águila-Carrasco, T. Ferrer-Blasco, and R. Montés-Micó, "Effect of large apertures on the optical quality of three multifocal lenses," *J. Refract. Surg.* **31**(10), 666–676 (2015).
20. A. Domínguez-Vicent, J. J. Esteve-Taboada, A. J. Del Águila-Carrasco, T. Ferrer-Blasco, and R. Montés-Micó, "In vitro optical quality comparison between the Mini WELL Ready progressive multifocal and the TECNIS Symphony," *Graefes Arch. Clin. Exp. Ophthalmol.* **254**(7), 1387–1397 (2016).
21. H. A. Weeber, S. T. Meijer, and P. A. Piers, "Extending the range of vision using diffractive intraocular lens technology," *J. Cataract Refract. Surg.* **41**(12), 2746–2754 (2015).
22. Abbott Medical Optics, <https://www.vision.abbott>.
23. International Organization for Standardization, ISO 11979–2:2014 "Ophthalmic Implants - Intraocular Lenses - Part 2: Optical Properties and Test Methods." Geneva; ISO; 2014.
24. Thorlabs, Inc., <https://www.thorlabs.com>.
25. L. N. Thibos, X. Hong, A. Bradley, and R. A. Applegate, "Accuracy and precision of objective refraction from wavefront aberrations," *J. Vis.* **4**(4), 329–351 (2004).
26. Z. Zalevsky, "Extended depth of focus imaging: a review," *J. of Photonics for Energy* 018001 (2010).

## 1. Introduction

In cataract surgery, an intraocular lens (IOL) replaces the natural crystalline lens. IOL power calculations of monofocal implants commonly target distinct distance vision. However, visual requirements at closer distances cannot be satisfied by monofocals and, similarly to the case of presbyopia, patients become spectacle dependent to perform their ordinary activity. Multifocal IOLs offer one (bifocals) or two (trifocals) additional focusing distances for near and intermediate vision. Diffractive multifocal IOLs (more precisely, refractive-diffractive multifocal IOLs) are based on the simultaneous image forming principle for which an in-focus image formed by one focus is overlaid by one or more secondary out-of-focus images formed by the other foci. This effect has an impact on the image contrast and is among the causes of dysphotopsia (such as halo and glare) reported by implanted patients. Recently, IOL designs based on extending the range of focus have been proposed to address the issue. Ideally, an extended-depth-of-focus (EDOF) lens produces a long and narrow focal segment in the image domain. An IOL of such a design would allow imaging in a continuous range of vision. The assessment of the IOL optical quality is conducted using optical and clinical methods. Optical bench testing of IOLs is objective, patient independent, and complementary to clinical assessment. The study and interpretation of both sorts of outcomes lead to clarify the characteristics of IOL designs with higher impact on vision and, hence, offer useful information to surgeons for implant selection and to designers for IOL optimization.

Diffractive bifocal intraocular lenses have a hybrid diffractive-refractive design that consists of a high-power refractive lens (carrier or base lens) and an additional (add) low-power diffractive profile engraved on either the front or the back surface of the IOL following a sawtooth pattern of echelettes. The optical path difference (OPD) for rays travelling through each zone, between the inner and outer step edges, is commonly expressed in terms of the design wavelength ( $\lambda_0$ ) or, equivalently, of the phase shift ( $\phi_0$ ) introduced in a light wavefront. So far, most of the diffractive profiles mainly utilize the zeroth and first diffraction orders to make the intraocular lens ( $(0^{\text{th}}, 1^{\text{st}})$ DIOL) form two images: distance and near images, respectively [1,2]. For the distance image, the  $0^{\text{th}}$  order energy goes to the image formed by the high-power refractive carrier lens, whereas the  $1^{\text{st}}$  order energy goes to the near image formed by the combined carrier plus add powers. The distribution of the energy between these diffraction orders - and hence, between the distance and near images- can be

properly adjusted by setting the step height of the profile. For example, if the diffractive steps are  $\pi$ -phase shift, meaning  $OPD = \lambda_0 / 2$  and  $\phi_0 = \pi$ , light will distribute ideally balanced between the two images (with theoretically 40.5% of energy efficiency each). Phase steps in the range  $0 < \phi_0 < \pi$  benefit the 0<sup>th</sup> order at the expense of the 1<sup>st</sup> order whereas phase steps in the range  $\pi < \phi_0 < 2\pi$  have the opposite effect. Moreover, apodized IOLs use gradual reduction of the step height to continuously modulate the phase shift from center to periphery. As a result, the energy distribution between the 0<sup>th</sup> and 1<sup>st</sup> order foci becomes pupil dependent [3]. These properties have been exploited in a variety of bifocal diffractive IOL designs studied elsewhere (see, for instance, studies using computational and/or on optical bench techniques [2,4,5], clinical studies assessing the impact on visual function [6] or both [7,8]).

Recently, chromatic aberration has drawn increasing attention in IOL design and visual optics research (see, for instance, Refs. 9–12). A diffractive profile with  $m2\pi$  maximum phase modulation –  $m$  being an integer number- operates at higher harmonic orders [13–15] and has proved to show interesting properties for achieving an effective reduction of the chromatic aberration that would otherwise affect severely common 1<sup>st</sup>-diffractive order lenses. Harmonic diffractive lenses with phase shift being an odd multiple of  $\pi$  (or, equivalently,  $OPD$  being an odd multiple of  $\lambda_0 / 2$ ) also direct light between two neighbor diffraction order images (with 40.5% energy efficiency each). Thus, for instance, a  $3\pi$ -phase-shift ( $OPD = 1.5\lambda_0$ ) diffractive lens distributes light between the 1<sup>st</sup> and 2<sup>nd</sup> diffraction orders with balanced energy [16]. If such a diffractive pattern is cut onto the base curve of a refractive carrier lens, the combined optical element will become a bifocal lens. If this combined element is meant to be an IOL, the carrier refractive and the diffractive powers must be carefully calculated to provide a range for distinct vision. A low addition diffractive bifocal IOL –typically with diffractive add power  $< 2$  D- would provide distinct vision at far and intermediate distances. Its near focus would actually provide distinct intermediate vision and for this reason we call it intermediate focus (instead of near focus) hereafter.

In this work, we describe analytically a hybrid refractive-diffractive IOL design named (1<sup>st</sup>,2<sup>nd</sup>)DIOL that operates with the 1<sup>st</sup> and 2<sup>nd</sup> diffractive orders, and prove experimentally its imaging properties on optical bench. An example of (1<sup>st</sup>,2<sup>nd</sup>)DIOL implementation can be found in the Tecnis Symphony ZXR00 IOL [Abbott Medical Optics, Abbott Park, IL]. This lens, henceforth the Symphony lens, has been introduced on the market with a patented novelty [17], as mentioned in Ref.18. As far as we know, this is the first time that the properties of a (1<sup>st</sup>,2<sup>nd</sup>)DIOL model are used to explain mathematically the chromatic performance of the Symphony lens. The verification of this hypothesis, both analytical and experimentally, constitutes an important objective of this work. The explanation is fully supported by the results of the experiment conducted to measure the red (R), green (G) and blue (B) through-focus energy efficiency (TF-EE) and the longitudinal chromatic aberration (LCA) of the foci.

For the sake of comparison, the experimental results obtained with a Symphony IOL are shown along with others corresponding to a monofocal (Tecnis ZA9003) IOL and a bifocal (0<sup>th</sup>,1<sup>st</sup>)DIOL (Tecnis ZKB00) of the same distance power. We review in this paper the mathematics concerning (0<sup>th</sup>,1<sup>st</sup>)- and (1<sup>st</sup>,2<sup>nd</sup>)- DIOLs. This leads us to discuss on bifocal design, Symphony's lens EDOF design, and on the compensation of chromatic aberration. Such results and discussions provide an additional context to the modulation transfer function based results recently reported by related research [18–21].

## 2. Materials and methods

### 2.1 Optical power and energy efficiency of a hybrid refractive-diffractive IOL

We assume a model for a hybrid refractive-diffractive IOL, according to which a thin carrier lens of refractive index  $n_l(\lambda)$  with a diffractive lens profile cut on one side [2] is immersed

in a medium of refractive index  $n_A(\lambda)$ , which represents both the aqueous and vitreous humors. The optical power  $P$  of such hybrid refractive-diffractive IOL, at a specific design wavelength  $\lambda_0$ , results from the addition of two terms, the refractive  $P_r$  and the diffractive  $P_d$  powers,

$$P(\lambda_0) = P_r(\lambda_0) + P_d(\lambda_0). \quad (1)$$

We assume in Eq. (1) that the lens thickness is negligible in comparison with the focal lengths involved. The power of the base refractive lens, with front  $R_1$  and back  $R_2$  radii, is

$$P_r(\lambda) = (n_L(\lambda) - n_A(\lambda)) [1/R_1 - 1/R_2]. \quad (2)$$

The diffractive profile, designed at wavelength  $\lambda_0$ , induces a phase shift ( $\phi_0$ ) at every step edge that is proportional to its height ( $h$ ), according to the expression

$$\phi_0 = \frac{2\pi}{\lambda_0} (n_L(\lambda_0) - n_A(\lambda_0))h. \quad (3)$$

The diffractive lens contributes with some of its  $m$  diffracted order powers

$$P_d(\lambda_0, m) = mP_d(\lambda_0, 1) \quad (4)$$

to the total IOL power (Eq. (1)). It is worth noticing that, according to Eq. (4), the 0<sup>th</sup> diffraction order ( $m = 0$ ) has null power. Let us assume that the step height of the diffractive lens produces an OPD of  $p\lambda_0$ , with  $p = (n_L(\lambda_0) - n_A(\lambda_0))h / \lambda_0$ , equivalent to a phase shift of  $p2\pi$  rad. When ( $p = 1$ ) a widely known result is obtained: the diffractive lens, illuminated with the design wavelength, reaches maximum efficiency, ideally 100%, in its positive 1<sup>st</sup> order while the other orders vanish. The power of the diffractive lens is  $P_d(\lambda_0, 1) = 2\lambda_0 / r_1^2$  with  $r_1$  denoting the radius of the first zone or central echelette.

For an illumination wavelength  $\lambda$  the diffraction energy efficiency of the  $m$  order is

$$\eta_m = \text{sinc}^2(\alpha p - m), \quad (5)$$

where  $\text{sinc } x = \sin(\pi x) / \pi x$  and  $\alpha$  is defined as the fraction of  $2\pi$  phase shift introduced for illumination wavelengths other than  $\lambda_0$ . In the context of the eye,  $\alpha$  is given by

$$\alpha = \frac{\lambda_0}{\lambda} \left[ \frac{n_L(\lambda) - n_A(\lambda)}{n_L(\lambda_0) - n_A(\lambda_0)} \right]. \quad (6)$$

In Eq. (6), the factor in brackets accounts for the little influence of material dispersion and hence, Eq. (6) is frequently approximated by  $\alpha \approx \lambda_0 / \lambda$ , with material dispersion neglected (see, for instance, Refs. 5,13). At wavelengths away from the design  $\lambda_0$ , the power of each diffractive order  $m$  follows the equation

$$P_d(\lambda, m) = \frac{m\lambda}{\lambda_0} P_d(\lambda_0, 1), \quad (7)$$

but their diffracted energy efficiency –given by Eq. (5)– falls quickly (except for the harmonic wavelengths, that is, those that satisfy  $\lambda_n = p\lambda_0 / m$ , which come to a common focus with the design wavelength and with same high efficiency [13,14]).

## 2.2 Longitudinal chromatic aberration in a 1<sup>st</sup> and 2<sup>nd</sup> diffractive order IOL

For non-integer values of  $p$ , let us say  $m < p < m + 1$  (with  $m$  integer), light mainly distributes between the two adjacent  $m$  and  $m + 1$  diffraction orders. This is, among other examples, the mentioned case of  $p = 0.5$ , with light split and mostly directed to the 0<sup>th</sup> and 1<sup>st</sup> orders, and also the case of  $p = 1.5$ , with light mostly directed to the 1<sup>st</sup> and 2<sup>nd</sup> orders [2,14,16].

At any focus of a hybrid refractive-diffractive IOL, the optical power variation with illuminating wavelength  $\lambda$  -and hence, LCA- results from the addition of two terms that account for: one, the dispersive nature of the optical materials through their refractive indexes  $n(\lambda)$  and two, the inherent spectral properties of the diffraction orders involved. Typically, LCA measures optical power variation  $\Delta P(\lambda)$  along the optical axis in the image space (although it can be equivalently translated to the object space). Thus, each focus of a hybrid refractive-diffractive IOL, which is formed by the joint contribution of the base refractive lens power and a specific  $m$ -diffraction order, shows a LCA that can be written as

$$\text{LCA}(m) = \Delta P_r + \Delta P_d(m), \quad (8)$$

where subindexes  $r$ ,  $d$  stand for refractive and diffractive contributions, respectively. The refractive power variation of the carrier lens  $\Delta P_r$  is usually referred to {Fdc} set of wavelengths, with  $\lambda_f = 486\text{nm}$ ,  $\lambda_d = 588\text{nm}$ , and  $\lambda_c = 656\text{nm}$ , for which the coefficient of refractive dispersion named Abbe number is defined as  $V = \frac{n(\lambda_d) - 1}{n(\lambda_f) - n(\lambda_c)}$ . The refractive power variation  $\Delta P_r$  can be calculated using the mathematical expression [12]

$$\Delta P_r \{\text{Fdc}\} = P_r(\lambda_f) - P_r(\lambda_c) = \left[ \left( \frac{n_L(\lambda_d) - 1}{V_L} \right) - \left( \frac{n_A(\lambda_d) - 1}{V_A} \right) \right] \frac{P_r(\lambda_d)}{n_L(\lambda_d) - n_A(\lambda_d)}, \quad (9)$$

where the refractive power of the lens for wavelength  $\lambda$  is given by Eq. (2).

The diffractive lens power change with wavelength can be obtained from Eq. (7), so that

$$\Delta P_d(\lambda_0, m) = -m \frac{\Delta \lambda}{\lambda_0} P_d(\lambda_0, 1), \quad (10)$$

with  $\Delta \lambda$  commonly limited to the visible spectral range. The negative sign in Eq. (10) accounts for a power variation in the opposite direction to that produced by the refractive lens (Eq. (9)). The step height of the profile plays an essential role in the contribution of the diffractive lens to the LCA of the IOL. To illustrate this effect with an example, let us consider a (0<sup>th</sup>, 1<sup>st</sup>)DIOL, that is, a hybrid refractive-diffractive IOL with step height producing a  $\pi$ -phase shift in the design wavelength  $\lambda_0$ . As mentioned, this lens performs bifocally with balanced efficiency at that wavelength between the 0<sup>th</sup> and 1<sup>st</sup> diffraction orders, which are associated to the distance and near IOL powers, respectively. Since the 0<sup>th</sup> order has null power (Eq. (4)), the LCA at the distance focus is computed using Eq. (8) with  $m = 0$ ,

$$\text{LCA}_{\text{distance}} \{(0^{\text{th}}, 1^{\text{st}})\text{DIOL}\} = \Delta P_r(\lambda_0), \quad (11)$$

which means that the chromatic aberration in the distance focus depends entirely on the refractive base lens. To obtain LCA in the near focus, we take Eq. (8) with  $m = 1$ , which involves the contribution of the diffractive lens operating in the 1<sup>st</sup> order

$$\text{LCA}_{\text{near}} \{(0^{\text{th}}, 1^{\text{st}})\text{DIOL}\} = \Delta P_r(\lambda_0) + \Delta P_d(\lambda_0, 1), \quad (12)$$

and  $\Delta P_d(\lambda_0, 1) = -P_d(\lambda_0, 1)\Delta\lambda / \lambda_0$  as derived from Eq. (10) for the 1<sup>st</sup> diffraction order. We recall that Eq. (12) will be also valid for an intermediate focus provided the diffractive power value is sufficiently low.

Let us compare the conventional (0<sup>th</sup>, 1<sup>st</sup>)DIOL with a lens designed to operate with the 1<sup>st</sup> and 2<sup>nd</sup> diffraction orders to provide the distance and near (intermediate) foci. We will show that this design leads to significant differences regarding power and spectral performance. For the sake of simplicity, we keep the term “near” along the explanation, but it could be replaced by “intermediate” depending on the value of the diffractive power. According to Eqs. (1), (2) and Eqs. (4), (5), the distance and near powers of such (1<sup>st</sup>, 2<sup>nd</sup>)DIOL for the design wavelength are

$$P_{\text{distance}} \{(1^{\text{st}}, 2^{\text{nd}})\text{DIOL}, \lambda_0\} = P_r(\lambda_0) + P_d(\lambda_0, 1), \quad (13)$$

$$P_{\text{near}} \{(1^{\text{st}}, 2^{\text{nd}})\text{DIOL}, \lambda_0\} = P_r(\lambda_0) + 2P_d(\lambda_0, 1), \quad (14)$$

and both have balanced efficiency of 40.5% at  $\lambda_0$ . According to Eqs. (8), (10), their LCAs are

$$\text{LCA}_{\text{distance}} \{(1^{\text{st}}, 2^{\text{nd}})\text{DIOL}\} = \Delta P_r(\lambda_0) - \frac{\Delta\lambda}{\lambda_0} P_d(\lambda_0, 1), \quad (15)$$

$$\text{LCA}_{\text{near}} \{(1^{\text{st}}, 2^{\text{nd}})\text{DIOL}\} = \Delta P_r(\lambda_0) - 2\frac{\Delta\lambda}{\lambda_0} P_d(\lambda_0, 1), \quad (16)$$

which means that the distance and the near powers, as well as the LCAs in both foci, depend on both the carrier refractive lens and the diffractive lens characteristics. Since the LCAs of the refractive and diffractive contributions have opposite sign, it implies that some compensation of the chromatic aberration can be expected for both the distance and the near foci. This fact clearly differs from the (0<sup>th</sup>, 1<sup>st</sup>)DIOL design (see Eqs. (11), (12)), for which, such compensation is only possible in the near focus but not in the distance focus [12]. We recall that Eqs. (11), (12), (15), (16) refer, exclusively, to the LCA introduced by the IOL and do not take into account the contributions of the cornea and other ocular media to the LCA of the eye.

Since the LCA produced by diffractive components depends linearly on the wavelength difference and the diffractive order (Eq. (10)), some care must be taken regarding the near focus in a (1<sup>st</sup>, 2<sup>nd</sup>)DIOL. As Eqs. (15), (16) reveal, the compensation of chromatic aberration in the near focus doubles the compensation in the distance focus. For example, if the refractive power variation were fully compensated in the distance focus, it would be overcompensated in the near focus, thus producing an undesired chromatic aberration in it. Fortunately, this effect can be mitigated by three factors. First, the diffraction efficiency, governed by Eq. (5); second, the add power of the diffractive lens,  $P_d(\lambda_0, 1)$ , which is generally much lower than the power of the base refractive lens (about 10% in diopters), and third, the possibility of apodization. Step height reduction from center to periphery, benefits 1<sup>st</sup> order efficiency, as pupil size increases, at expenses of the 2<sup>nd</sup>. A good design must reach a trade-off with all these factors.

### 2.3 Intraocular lenses

Three Tecnis (Abbott Medical Optics, Abbott Park, IL) IOLs were used in the experiment: a Symphony ZXR00 (Fig. 1), a bifocal ZKB00, and a monofocal ZA9003. All three IOLs shared the same material and had the same aspheric design of the refractive base lens. They had similar power for distance vision (30D). The first two were hybrid refractive-diffractive designs. The monofocal IOL, with purely refractive design, was included as a reference in the

study. Further IOL specifications and features are listed in Table 1. The diffractive design of Tecnis ZKB00, with + 2.75 D add power, is intended to produce a balanced distribution of energy between the distance and the near foci independently of the pupil diameter.

**Table 1. Optical data of Tecnis (Abbott Medical Optics) intraocular lenses<sup>a</sup>**

	Symphony ZXR00	ZKB00	ZA9003
Material		Hydrophobic Acrylic	
Refractive index $n$	1.47	1.47	1.47
Abbe value $V$	55	55	55
Color filter	UV-blocking	UV-blocking	UV-blocking
Optic Zone diameter (mm)	6	6	6
Aspheric surface <sup>b</sup>	Anterior	Anterior	Anterior
$SA = c[4,0]$ ( $\mu\text{m}$ ) <sup>c</sup>	-0.27	-0.27	-0.27
Diffractive design	Pupil-dependent	Full-aperture	NA <sup>d</sup>
	Posterior	Posterior	
Base Power (D)	30	30	30
Add Power (D) at IOL plane	+ 1.75	+ 2.75	NA <sup>d</sup>

<sup>a</sup>Specifications provided by the manufacturer for wavelength of 555 nm and 37°C [22]. <sup>b</sup>Data for a 6mm pupil; <sup>c</sup>SA, spherical aberration; <sup>d</sup>NA, not applicable.

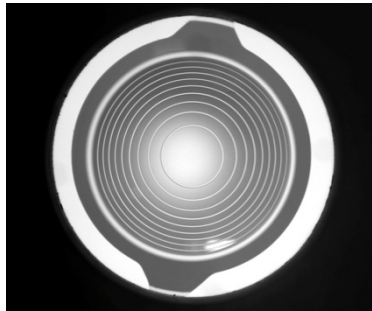


Fig. 1. Symphony IOL tested in the work. Measured values for ring diameter and step height are listed in Table 2.

**Table 2. Data of the Tecnis Symphony ZXR00 IOL (30D)**

Echelette/Ring	Step Height ( $\mu\text{m}$ )		Outer diameter (mm)		OPD ( $\lambda_0$ units)
	Design <sup>a</sup>	Experimental <sup>b</sup> ( $\pm 0.2$ )	Design <sup>a</sup>	Experimental <sup>c</sup> ( $\pm 0.01$ )	
1	6.2	NA	1.60	1.57	1.5
2	6.2	6.3	2.20	2.21	1.5
3	6.2	6.2	2.75	2.72	1.5
4	5.6	5.5	3.17	3.14	1.366
5	5.6	5.7	3.55	3.53	1.366
6	5.6	5.8	3.88	3.86	1.366
7	5.6	NA <sup>d</sup>	4.20	4.19	1.366
8	5.6	NA	4.48	4.46	1.366
9	5.6	NA	4.76	4.74	1.366

<sup>a</sup>From exemplary diffractive profile, according to an embodiment of the invention described in Ref.17; <sup>b</sup>Measured with confocal microscope (PL $\mu$  Sensofar) and 100x objective; <sup>c</sup>Measured from the digital image captured by the microscope and camera of the setup; <sup>d</sup>NA, not available.

The Symphony ZXR00 IOL is claimed to be designed with a proprietary method based on a combination of refractive and diffractive technologies for providing EDOF and, therefore, extended range of vision with combined correction of spherical and chromatic aberration [21] for contrast sensitivity enhancement [10]. Valuable information is provided in Ref.21 concerning the principles used in design of the IOL diffractive profile: embedded echelettes for offset phase correction with respect to the baseline of the refractive lens [2] and multiple echelettes for EDOF with chromatic correction, but the authors do not mention the specific diffractive orders used for the lens design. Although further details describing the patented

technology can be found out in Ref.17, it is not straightforward from this information to assign a specific diffractive design to the Symphony lens and hence, to fully understand the physical mechanisms of its performance.

We have measured ring diameter and step height of the central zones of the diffractive profile of the Symphony lens used in our study (Fig. 1) with confocal microscopy. For the sake of comparison, Table 2 contains these measurements along with the values corresponding to an exemplary diffractive profile, according to an embodiment of the invention described in Ref. 17. Let us remark the good agreement between the design and measured values. The exemplary profile includes OPD in terms of the design wavelength  $\lambda_0$  and the intended light distribution between the 1<sup>st</sup> and 2<sup>nd</sup> diffraction orders. Some parameters considered in the exemplary profile calculation were the refractive index of the aqueous of the eye (1.336), the refractive index (1.47) of the ophthalmic lens material and the design wavelength (550 nm approximately) which is within the range  $546 \pm 10\text{nm}$  recommended by ISO 11979-2:2014 [23]. According to the description, the diffractive profile consists of two main regions: central and peripheral. The central zone includes echelettes of  $3\pi$ -phase shift steps ( $\text{OPD} = 1.5\lambda_0$ ) that ideally deviate similar amount of energy (40.5%) to the 1<sup>st</sup> and 2<sup>nd</sup> diffraction orders for balanced 50:50 energy distribution. The peripheral zone includes echelettes of  $2.732\pi$ -phase shift steps ( $\text{OPD} = 1.366\lambda_0$ ) that ideally deviate 63% of energy to the 1<sup>st</sup> diffraction order and 21% to the 2<sup>nd</sup> one for 75:25 energy distribution. The base refractive power plus the 1<sup>st</sup> diffraction order direct a fraction of the incoming light to the distance focus while another fraction is directed to another focus, to which the base refractive power and the 2<sup>nd</sup> diffractive order contribute. The latter is called intermediate focus because of its low addition (+ 1.75 D) [17].

The 0<sup>th</sup> order would not be used for imaging purposes and about 16% to 18% of the incoming light would be diverted to spurious diffractive orders [17]. The OPD increase introduced by central echelettes -from  $0.5\lambda_0$  in many conventional bifocals to the current  $1.5\lambda_0$  in the Symphony lens- would be specifically intended to compensate for chromatic aberration. For pupils within the central region, EDOF effect would be produced by central echelettes with balanced light distribution between the distance and intermediate foci; for larger pupils covering the central and part of the peripheral regions, peripheral echelettes would benefit the distance focus.

Taking into account the diameter and step height measurements as well as other parameters of the Symphony lens contained in Tables 1 and 2, we reasonably postulate that Symphony IOL may represent an example of (1<sup>st</sup>,2<sup>nd</sup>)DIOL. The verification of this hypothesis, both analytical and experimentally, constitutes an important objective of this work.

#### 2.4 Experimental setup and metrics

The experimental setup was arranged on optical bench. Three LEDs with emission in the blue (B), green (G) and red (R) spectral bands (Table 3) illuminated the setup sequentially. We measured the R, G, B through-focus energy efficiency (TF-EE) of each IOL. The focus powers and their corresponding LCA were experimentally obtained in all lenses from the R, G, B TF-EE curves. For comparison, mathematical estimations of these magnitudes have been calculated using Eq. (5) and Eqs. (11) to (16). Each IOL was introduced in a wet cell with parallel windows. The optical setup was similar to that used by the authors in related works and described in detail elsewhere (Ref. 12 and, except for the artificial cornea, Ref. 4).

The TF-EE is the quality metrics we have used in this work to test the IOLs under R, G, B illumination. It is worth remarking that the energy efficiency (EE) values of the distance and near foci were straightforwardly obtained from dense sampling the through-focus scan, particularly in the axial neighborhood of focal planes. The same test was repeated for the reference monofocal IOL, but referred to its single (distance) focus.

The method used to measure the EE in the image space has been reported in detail in former works for one [4] or more wavelengths [12]. It includes a pinhole object at infinity and



a microscope plus a camera for digital image acquisition. The method firstly applies an edge detection algorithm to segment the central core of the pinhole image at the focus plane of the lens. It secondly quantifies the amount of light intensity in the core ( $I_{core}$ ) relative to the intensity in the full image that comprises the core and the background ( $I_{total} = I_{core} + I_{background}$ ). The EE is given by the ratio  $I_{core} / I_{total}$ , which is easy to compute in the experimental practice and approaches the so-called light-in-the-bucket metric [25]. From definition, the light-in-the bucket metric captures the diffraction energy efficiency of IOL as well as image blur caused by aberrations and scattering. It quantifies the amount of light in the central core of the point spread function (PSF) relative to that in a monofocal diffraction-limited PSF for the same wavelength and pupil size [5]. The implementation of this metric in the experimental practice, for which the ideal point source is replaced by a pinhole of certain size, has been described and justified in a former work [12].

Table 3. Spectral data of LEDs<sup>a</sup>

Light		$\lambda$ (nm)	FWHM <sup>b</sup> (nm)	$\alpha \approx \frac{\lambda_0}{\lambda} c$
$\lambda_0$	Design wavelength	550		1
	<b>Manufacture model</b>			
B	Thorlabs M455L3-LED	455	$\pm 10$	1.209
G	Thorlabs M530L3-LED	530	$\pm 20$	1.038
R	Thorlabs M625L3-LED	625	$\pm 10$	0.880

<sup>a</sup>Nominal data from Thorlabs (see Ref.24); <sup>b</sup>Full width at half maximum; <sup>c</sup>Phase delay fraction.

During the through-focus test, the core contour determined in the best focus plane was applied with no change to the defocus images obtained by scanning neighbor planes. Axial scanning was stretched to cover the segment of interest in case of multifocal or EDOF IOLs, including the distance and near (intermediate) foci.

A TF-EE curve was experimentally obtained for each IOL under study and every R, G, and B light. Through-focus measurements were taken in the IOL image space and covered about 7 D in 0.2 D steps. For more precision, double density sampling was used when testing the Symphony lens with 2.2mm pupil. LCA experimental values were obtained from the power difference between the furthest EE peaks (corresponding to R and B) at each focus plane.

The experimental work of this study has been done using the setup described elsewhere [12] and summarized here for the sake of conciseness. A 200-micron pinhole test object was placed at the front focal plane of a collimating lens of 200-mm focal length. The collimated beam illuminated the wet cell where the IOL was inserted and thus, one or two aerial images of the pinhole object, or a focal segment, were formed behind the wet cell depending on the lens design. A diaphragm, placed in front of the wet cell and used as entrance pupil, limited the IOL aperture to 3.5 mm diameter during most part of the experiment. With this pupil the impact of the negative spherical aberration of all tested IOLs on their images was still relatively low, which helped us to compute the light-in-the bucket metric. The Symphony IOL was additionally tested with an entrance pupil of 2.2mm that limited its aperture to two central echelettes (Table 2). Behind the wet cell an infinite corrected microscope focused the aerial image of interest and magnified it onto a monochrome 8-bit CCD camera for digital image acquisition. The set of microscope and camera was mounted on a translation holder for axial scanning and moved away along the bench axis with spatial resolution of  $\pm 1$  micron. For every IOL and R,G,B light, the intensity of the LED source and the time integration of image acquisition were adjusted to obtain a linear response of the camera in the intensity range of the aerial images (from distance to near images) with no saturation of the camera sensor.

### 3. Results

Figure 2 shows the experimental TF-EE curves measured for the monofocal (a) and bifocal (b) IOLs with a pupil size of 3.5mm under R, G, and B LED lights. Power and energy efficiency peak values, and LCA are listed in Table 4. A first explanation of these results can be found in a former work [12].

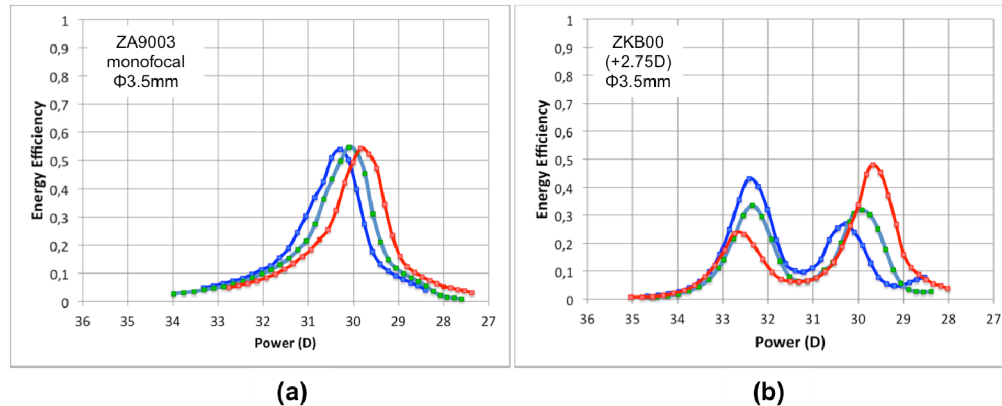


Fig. 2. Experimental TF-EE curves of 30D Tecnis monofocal ZA9003 and bifocal ZKB00 (+ 2.75D) IOLs obtained *in-vitro* under R (solid red line), G (solid green line) and B (solid blue line) LED lights. Small squares represent experimental measurements.

**Table 4. Power, energy efficiency and LCA measured for Tecnis ZA9003 and ZKB00 (+ 2.75 D) IOLs<sup>a</sup>**

$\lambda$	Tecnis Monofocal ZA9003			Tecnis Bifocal ZKB00 + 2.75 (with OPD = 0.5 $\lambda_0$ )				
	Power (D)	Energy efficiency	Power (D)		Energy efficiency			
			Distance focus $m = 0$	Near focus $m = 1$	Distance focus $m = 0$	Near focus $m = 1$	Distance/Near Ratio	
$\lambda_0$	550	(30.0)		(30.00)	(32.75)	(0.41)	(0.41)	(1)
B	455	<b>30.29</b>	<b>0.54</b>	<b>30.26</b>	<b>32.42</b>	<b>0.27</b> (0.25)	<b>0.43</b> (0.58)	<b>0.62</b> (0.43)
G	530	<b>30.10</b>	<b>0.55</b>	<b>30.10</b>	<b>32.34</b>	<b>0.32</b> (0.38)	<b>0.34</b> (0.44)	<b>0.95</b> (0.86)
R	625	<b>29.83</b>	<b>0.54</b>	<b>29.68</b>	<b>32.74</b>	<b>0.48</b> (0.51)	<b>0.24</b> (0.31)	<b>2.04</b> (1.62)
LCA		<b>0.46</b>		<b>0.58</b>	<b>-0.32</b> (-0.27)			

<sup>a</sup>Nominal specifications and theoretical estimations of LCA and diffraction energy efficiency  $\eta$  are included in brackets, below the experimental values, for comparison.

The monofocal IOL (Fig. 2(a)) shows a single focus for distance vision and hence, only one efficiency peak under each R, G and B illumination. The RGB TF-EE curves of the monofocal IOL are very similar and close to each other, with the G peak centered at about 30 D, which is the nominal power for the design wavelength (550nm). The B and R peaks are separated away LCA = 0.46D (Table 4) and placed at either side of the G peak. The bifocal ZKB00(+ 2.75D) IOL (Fig. 2(b)) has hybrid refractive-diffractive design with  $p = 0.5$  and hence, it shows two foci, for distance and near vision, that correspond to the 0<sup>th</sup> and 1<sup>st</sup> diffraction orders, respectively. With G illumination, the closest to the design wavelength, the TF-EE curve shows quite balanced energy distribution between distance and near foci, with peak EE values of 0.32 (distance) and 0.34 (near) that are slightly below the estimated theoretically diffraction efficiency (0.38 for distance and 0.44 for near) (Table 4). The B and R curves of the bifocal show two peaks as well, but with opposite variations in EE as

expected from the wavelength dependence of the diffraction efficiency (Eq. (5)). The LCA in the distance focus of the bifocal (0.58D) has the refractive contribution of the carrier lens (Eq. (11)) and, consequently, is very similar to the LCA obtained with the monofocal IOL (0.46D). The LCA in the near focus, however, is compensated in part by the contribution, with opposite sign, of the diffractive profile operating with the 1<sup>st</sup> diffraction order (Eq. (12)). Again, the LCA predicted theoretically for the near focus (−0.27D) is very close to the experimental value (−0.32 D). This interpretation, supported by the good agreement between the numerical estimations and the experimental results (Table 4), validates the (0<sup>th</sup>,1<sup>st</sup>)DIOL model developed for  $p = 0.5$  and orders  $m = \{0,1\}$  in Section 2 (see also Ref. 12).

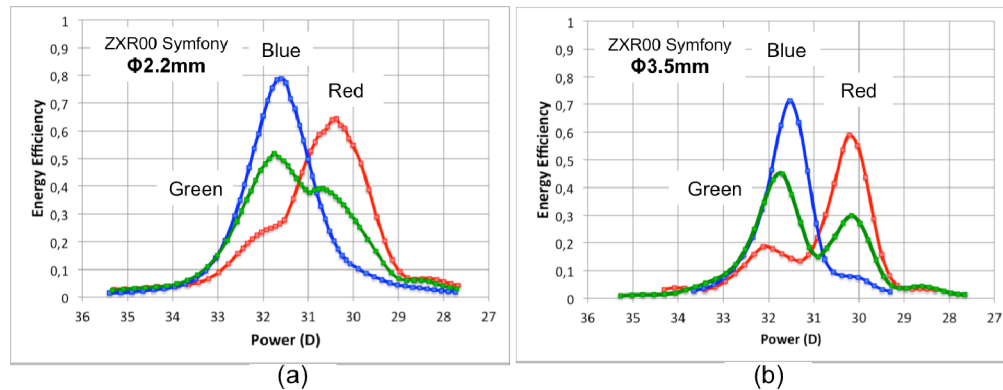


Fig. 3. Experimental TF-EE curves of 30D Tecnis Symphony ZXR00 IOL obtained *in-vitro* with (a) 2.2 mm pupil and (b) 3.5 mm pupil, under R (solid red line), G (solid green line) and B (solid blue line) LED lights. Small squares represent experimental measurements.

Figure 3 shows the experimental TF-EE curves measured for the Symphony lens for (a) 2.2 mm and (b) 3.5mm pupils under R, G, and B LED illumination. These curves differ quite significantly from those analyzed so far in this work. The B TF-EE curve has a single peak centered at about 31.5 D for both pupil sizes, being the peak obtained with the small 2.2mm aperture of larger full width at half maximum (FWHM) -about 50% larger- than the obtained with the 3.5mm aperture. The G TF-EE curve exhibits two separate peaks of different EE with 3.5mm pupil (Fig. 3(b)). The lowest, centered at about 30D, would correspond to the distance focus whereas the highest, centered at a power slightly below 32D, would correspond to the intermediate focus. Peak asymmetry is markedly prominent in the R TF-EE curve with 3.5mm pupil, but in the opposite direction to that shown by the G TF-EE curve. With 2.2mm pupil, however, the R and G TF-EE curves exhibit a single asymmetric wide peak with  $\text{FWHM} \geq 2 \text{ D}$ . The interpretation of these figures is not straightforward and, certainly, not possible in terms of the conventional bifocal (0<sup>th</sup>,1<sup>st</sup>)DIOL design.

#### 4. Discussion

The (1<sup>st</sup>, 2<sup>nd</sup>)DIOL design, as introduced in Section 2, is still a bifocal lens that may feature good properties in chromatic compensation and depth of focus extension when it uses low addition power. Other solutions for depth of focus extension have been proposed and described elsewhere (see, for instance, a review in Ref. 26).

Let us interpret the results shown in Fig. 3 for the Symphony IOL in the light of an optical design based on a 1<sup>st</sup> and 2<sup>nd</sup> diffractive order profile, with the term “near” replaced by “intermediate” to account for the relatively low add value (+ 1.75 D). Table 5 contains the results of the calculations obtained using Eqs. (1)–(16) with  $\lambda_0 = 550\text{nm}$ , step height factors  $p = \{1.5, 1.336\}$ , diffractive orders  $m = \{1, 2\}$ , and phase delay fractions for the R, G, B lights approached by  $\alpha \approx \lambda_0 / \lambda$  (Table 3) with material dispersion neglected. The first row of Table 5 shows the design values for the (1<sup>st</sup>, 2<sup>nd</sup>)DIOL: distance and intermediate powers ( $P_{\text{distance}} =$

30D,  $P_{\text{interm}} = 31.75\text{D}$ ), add power  $P_d(\lambda_0, 1) = 1.75\text{D}$  under  $\lambda_0$  illumination. From Eq. (13), the design refractive power of the carrier lens can be inferred, resulting  $P_r(\lambda_0) = 28.25\text{D}$ . The design intermediate power would add the 2<sup>nd</sup> diffraction order, which is  $P_d(\lambda_0, 2) = 3.5\text{D}$ , to the refractive power. Thus, using Eq. (14), it turns out  $P_{\text{interm}} = 31.75\text{D}$ , which satisfies the nominal power for intermediate focus.

**Table 5. Theoretical estimations for (1<sup>st</sup>,2<sup>nd</sup>)DIOL**

$\lambda$	Power (D)					Diffraction Energy Efficiency			
	Refract carrier $P_r$	1 <sup>st</sup> order $P_d(\lambda, 1)$	2 <sup>nd</sup> order $P_d(\lambda, 2)$	$P_{\text{distance}}$	$P_{\text{interm}}$	Center (OPD=1.5 $\lambda_0$ )		Peripheral (OPD=1.366 $\lambda_0$ )	
						Distance focus $\eta_1$	Interm. focus $\eta_2$	Distance focus $\eta_1$	Interm. focus $\eta_2$
$\lambda_0$	28.25	1.75	3.50	<b>30.00</b>	<b>31.75</b>	0.41	0.41	0.63	0.21
B	28.49	1.45	2.90	<b>29.93</b>	<b>31.38</b>	0.05	0.89	0.19	0.66
G	28.25	1.69	3.37	<b>29.94</b>	<b>31.62</b>	0.32	0.50	0.54	0.28
R	27.97	1.99	3.98	<b>29.96</b>	<b>31.94</b>	0.71	0.16	0.87	0.06
$\Delta P\{RGB\}$	+0.52	-0.54	-1.08						
<b>LCA</b>				<b>-0.02</b>	<b>-0.56</b>				

For the illumination with the R, G, B LEDs some assumptions can be made concerning the carrier refractive lens. First, the refractive power for the G light can be reasonably approximated by the design refractive power (i.e.  $P_r(G) \approx P_r(\lambda_0) = 28.25\text{D}$ ). Second, taking into account the design characteristics that the refractive carrier lens of the hybrid refractive-diffractive IOLs and the monofocal IOL of this work would have in common (see Tables 1 and 4) and although the refractive carrier of the Symphony lens would have a refractive power (28.25 D) somewhat lower than the other two (30 D), we assume that all three refractive designs would contribute similarly to LCA. Therefore, we assume 0.52 D for the chromatic power variation of the Symphony's refractive carrier, which averages the values measured in the distance focus of the bifocal (0.58 D) and the single focus of the monofocal (0.46 D) (Table 4). We scaled the refractive powers of the Symphony's carrier for B and R with respect to G light so as to produce a refractive contribution of 0.52 D to LCA. The resulting estimated values are  $P_r(B) = 28.49\text{D}$  and  $P_r(R) = 27.97\text{D}$  (Table 5). The 1<sup>st</sup> and 2<sup>nd</sup> order powers,  $P_d(\lambda, 1)$  and  $P_d(\lambda, 2)$ , for R, G, and B lights, have been calculated using Eq. (7), and the distance and intermediate powers with Eqs. (13), (14). The diffraction energy efficiency has been calculated using Eq. (5) for all wavelengths. The  $\Delta P$  row contains the RGB power variations of the refractive carrier lens ( $\Delta P_r = +0.52\text{D}$ ) and the diffractive profile ( $\Delta P_d(\lambda, 1) = -0.54\text{D}$ ,  $\Delta P_d(\lambda, 2) = -1.08\text{D}$ ). They contribute to the LCA by compensating each other in the distance and the intermediate foci. As a result, LCA would be almost suppressed in the distance focus ( $\text{LCA}_{\text{distance}} = -0.02\text{D}$ ) and would keep low ( $\text{LCA}_{\text{interm}} = -0.56\text{D}$ ) in the intermediate focus.

When the step height factor is  $p = 1.5$ , it is worth mentioning the low efficiency of the 2<sup>nd</sup> diffraction order for R light (0.16) and the very low 1<sup>st</sup> diffraction order for B light (0.05), thus predicting a shortage of these color lights in either the intermediate or the distance focus to which they contribute. Conversely, the 1<sup>st</sup> diffraction order with R light reaches high energy efficiency (0.71) and so does the 2<sup>nd</sup> diffraction order with B light, reaching even a higher value (0.89), thus predicting the importance of these color lights in the specific focus to which they contribute.

The estimations contained in Table 5 must be compared with the values experimentally obtained using the Symphony lens with 2.2mm aperture (Fig. 3(a)). According to the exemplary embodiment described in Ref. 17 and the outer diameters of the Symphony's

echelettes (Table 2), the 2.2mm aperture contains the two central echelettes, with  $p = 1.5$  ( $OPD = 1.5\lambda_0$ ) and diffractive orders  $m = \{1,2\}$ . At a glance, only the B TF-EE curve seems to agree with the estimations (Table 5), but the R and G TF-EE curves appear to differ significantly. However, if we analyze them in detail –as we are going to do– we will find that they are in very good agreement too. Certainly, due to the relative proximity of the distance and the intermediate foci –only 1.75D apart– and the effect of a small 2.2mm pupil, which involves inherent depth of focus extension, we may consider that both foci overlap on the optical axis and, as a result, the TF-EE curve becomes the envelope of the addition of the two distance and intermediate EE peaks. We illustrate this effect in Fig. 4, more specifically in Figs. 4(b) and 4(c). For simplicity, we have considered that the energy efficiency curve in the vicinity of a focus can be approached by a Gaussian function. We have fit the experimental R and G TF-EE curves to the addition (in solid black line) of two Gaussian functions (in dashed and dotted lines) that minimize the accumulated square error with respect to the experimental curve over the range of interest (solid black line's domain). The results in Figs. 4(b) and 4(c) show two Gaussian functions with different height, centered at the distance and intermediate foci. Their addition (solid black lines) fits the experimental curve with remarkable accuracy in either case. The B TF-EE curve was approached by a single Gaussian function corresponding to the intermediate focus. The central position and the maximum value of the obtained Gaussian functions correspond to the experimental power and energy efficiency of the R, G, and B distance and intermediate foci of the Symphony lens with 2.2mm pupil. In Table 6 we compare these values with the theoretical predictions taken from Table 5. The excellent agreement between theoretical estimations and experimental results for 2.2mm pupil (Table 6) confirms the validity of our analysis and interpretation of the RGB TF-EE curves of Fig. 3(a). Moreover, they allow us to experimentally prove that the central zone of the Symphony lens (two central echelettes within 2.2mm pupil) performs as (1<sup>st</sup>, 2<sup>nd</sup>)DIOL with low + 1.75D add power.

We have repeated this exercise for the experimental RGB TF-EE curves obtained with a 3.5mm pupil (Fig. 3(b)). In this case, the larger aperture of the pupil reduces the natural depth of focus, and hence, the peak mutual overlapping. The B TF-EE curve (Fig. 3(b)) shows a single intermediate focus with a very low plateau at the expected position of the distance focus. The R and G TF-EE curves show two asymmetric foci, placed at the distance and intermediate focus positions. Gaussian decompositions, similar to those presented in Fig. 4, have been calculated for the experimental RGB TF-EE measured with 3.5mm pupil although they are not plotted here for brevity. The corresponding center and maximum values appear in Table 6 to represent experimental power and energy efficiency values, respectively.

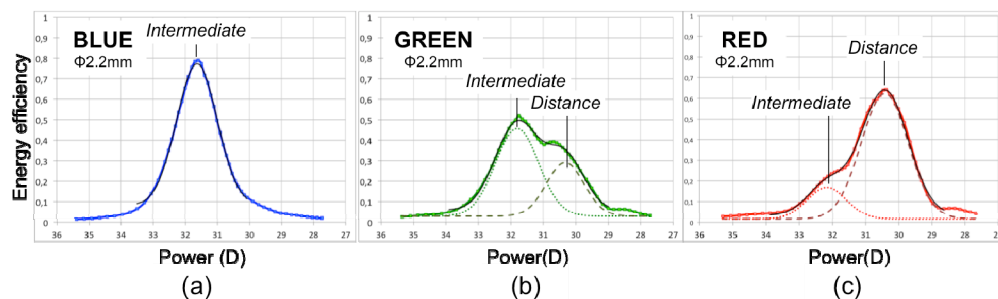


Fig. 4. Decomposition of (a) B, (b) G, and (c) R experimental TF-EE curves of Tecnis Symphony ZXR00 IOL (Fig. 3a) in terms of addition of Gaussian functions centered at the distance and intermediate foci: Experimental curve (thick solid line), fit function (black solid line) resulting from the addition of Gaussian functions centered at distance focus (dark dashed line) and intermediate focus (dotted line) that minimizes the cumulative square error over the range.

To further interpret the energy efficiency values obtained with a pupil of 3.5mm (Fig. 3(b)), we take into account that, according to the exemplary design described in Ref. 17 and the dimensions of the Symphony's echelettes (Table 2), two more echelettes (the 3<sup>rd</sup> and 4<sup>th</sup> ones) are also included when using a 3.5mm pupil. We recall that the 4<sup>th</sup> echelette lies in the peripheral region of the lens aperture, with  $p = 1.366$  ( $OPD = 1.366\lambda_0$ ). With 3.5mm pupil, the IOL was operating with 9.62 mm<sup>2</sup> aperture area, of which, 5.94mm<sup>2</sup> (61.7%) were corresponding to the first three echelettes, (with  $p = 1.5$ ) and 1.95mm<sup>2</sup> (20.3%) to the peripheral region (4<sup>th</sup> echelette, with  $p = 1.366$ ). Table 5 contains the diffraction energy efficiencies of the 1<sup>st</sup> and 2<sup>nd</sup> diffraction orders calculated for the peripheral echelettes with  $p = 1.366$ , under the illumination of  $\lambda_0$ , R, G, and B lights. The area covered by either the three central echelettes (61.7%) or the fourth echelette (20.3%) has been taken as weight to estimate the theoretical diffraction energy efficiencies of the RGB distance and intermediate foci, as well as the distance to intermediate efficiency ratio. The resulting theoretical estimations (Table 6) are in very good agreement with the corresponding experimental power and energy efficiencies computed from the Gaussian decomposition of the RGB TF-EE curves obtained with 3.5mm pupil.

Table 6. Tecnis Symphony ZXR00 IOL (30 D)<sup>a</sup>

POWER (D)									
$\lambda$	Distance focus			Intermediate focus			Cumulative Square Error		
	Theor estimation	Experimental		Theor estimation	Experimental		$\varnothing 2.2$	$\varnothing 3.5$	
		$\varnothing^b 2.2$	$\varnothing 3.5$		$\varnothing 2.2$	$\varnothing 3.5$			
$\lambda_0$	<b>30.00</b>			<b>31.75</b>					
B	<b>29.93</b>	–	30.13	<b>31.38</b>	31.63	31.54	0.0029	0.0004	
G	<b>29.94</b>	30.32	30.17	<b>31.62</b>	31.81	31.78	0.0027	0.0005	
R	<b>29.96</b>	30.42	30.19	<b>31.94</b>	32.17	31.91	0.0034	0.0026	
LCA	<b>-0.02</b>	Not eval.	-0.07	<b>-0.56</b>	-0.53	-0.37			

ENERGY EFFICIENCY												
$\lambda$	Distance focus				Intermediate focus				Distance/Intermediate Ratio			
	$\varnothing 2.2$		$\varnothing 3.5$		$\varnothing 2.2$		$\varnothing 3.5$		$\varnothing 2.2$		$\varnothing 3.5$	
	Theor $\eta$	Exper	Theor $\eta$	Exper	Theor $\eta$	Exper	Theor $\eta$	Exper	Theor $\eta$	Exper	Theor $\eta$	Exper
$\lambda_0$	<b>0.41</b>		<b>0.38</b>		<b>0.41</b>		<b>0.29</b>		<b>1</b>		<b>1.29</b>	
B	<b>0.05</b>	Negl.	<b>0.07</b>	0.07	<b>0.89</b>	0.77	<b>0.68</b>	0.70	<b>0.05</b>	Negl.	<b>0.10</b>	0.10
G	<b>0.32</b>	0.29	<b>0.31</b>	0.29	<b>0.50</b>	0.46	<b>0.36</b>	0.44	<b>0.63</b>	0.64	<b>0.84</b>	0.66
R	<b>0.71</b>	0.62	<b>0.61</b>	0.57	<b>0.16</b>	0.17	<b>0.11</b>	0.16	<b>4.52</b>	3.69	<b>5.68</b>	3.43

Cumulative Square Error ( $\varnothing 2.2$ ): 0.023  
Cumulative Square Error ( $\varnothing 3.5$ ): 0.012

<sup>a</sup>Experimental values calculated from the R, G, B TF-EE curves (Figs. 3, 4); <sup>b</sup> $\varnothing$  (mm).

We were dubious about considering the contribution of the 5<sup>th</sup> echelette because it was not fully covered by the 3.5mm pupil and could be also affected by the influence of small misalignments. We recalculated the RGB energy efficiencies of the distance and intermediate foci assuming the further contribution of the 5<sup>th</sup> echelette, but we obtained an accumulated square error of 0.068 with respect to the experimental values. Because this square error is higher than 0.012 (Table 6), obtained when assuming the first four echelettes, we concluded that the contribution of the 5<sup>th</sup> echelette could be discarded.

Let us highlight the excellent and very consistent agreement between the experimental values and the theoretical estimations for the distance and intermediate power values with both pupils (Table 6). The experimental results additionally confirm that LCA is negligible at the distance focus and very low (and negative) at the intermediate focus, as expected.

Finally, although LCA is almost extinguished in a (1<sup>st</sup>, 2<sup>nd</sup>)DIOL of low addition we point out the very strong asymmetry –much stronger than the already reported in conventional

bifocal ( $0^{\text{th}}$ ,  $1^{\text{st}}$ )DIOL [12]- between the energy efficiency peaks of B and R lights. For instance, a ( $1^{\text{st}}$ ,  $2^{\text{nd}}$ )DIOL such as the Symphony lens, with 3.5mm pupil (Table 6), has an experimental distance/intermediate EE ratio of 3.43 for R light versus a ratio of 0.10 for B light, away by far from the ideal 1.29 for the design wavelength. A bifocal ( $0^{\text{th}}$ ,  $1^{\text{st}}$ )DIOL such as ZKB00 (+ 2.75), however, with the same 3.5mm pupil (Table 4), has an experimental distance/intermediate EE ratio of 2.04 for R light versus a ratio of 0.62 for B light, still far but in lesser amount from the balanced 1.0 ideal value for the design wavelength. This increase in both the R and B TF-EE asymmetry could have an impact on the color image quality that deserves further evaluation in future work.

Although the results analyzed in this work were obtained for 30 D IOLs (Table 1), they are translatable to IOLs of different power (a 20-24 D range is common) and can be estimated using the equations provided in Sections 2.1 and 2.2.

## 5. Conclusions

The imaging properties of two hybrid refractive-diffractive IOLs with different diffractive designs have been analyzed within the common context of a refractive carrier combined with a diffractive lens that operates with two adjacent diffraction orders, either ( $0^{\text{th}}$ ,  $1^{\text{st}}$ ) or ( $1^{\text{st}}$ ,  $2^{\text{nd}}$ ).

We have reviewed the mathematics for the distance and intermediate/near powers, the energy efficiency, their variation for a wavelength other than  $\lambda_0$ , and LCA in each focus. An example of a  $1^{\text{st}}$  and  $2^{\text{nd}}$  order hybrid refractive-diffractive IOL design has been found in the Tecnis Symphony ZXR00 IOL and this pattern matching has been reported here for the first time. We have proved the imaging properties of such IOL design by numerical simulation and also experimentally by measuring in-vitro the TF-EE curves of the Symphony IOL for R, G, and B illuminations. Analogous TF-EE measurements, obtained for the Tecnis monofocal ZA9003 and bifocal ZKB00 (+ 2.75D) counterparts, have allowed us to compare the optical imaging properties of power and energy efficiency of all three lenses, not only between them but also with respect to theoretical predictions. An excellent agreement was obtained in all cases, thus giving a sound support to the analysis carried out and the IOL models considered.

The low add power (+ 1.75 D) of the tested ( $1^{\text{st}}$ ,  $2^{\text{nd}}$ )DIOL provides some focus extension from distance to intermediate vision with remarkable chromatic compensation. This chromatic compensation is almost complete in the distance focus and very relevant in the intermediate focus. This fact, along with the aspheric design of the refractive carrier lens, should contribute to enhance the imaging properties of the lens.

The relative energy efficiency between the distance and the intermediate foci is modulated by changing the echelette step height in two regions of the Symphony lens aperture: a central region that directs the design wavelength to both foci with balanced energy, and a peripheral region that benefits the distance focus.

Some limitations must be mentioned though. The add power (+ 1.75D) can be insufficient in some instances. Higher add powers could be considered as well but at the price of sacrificing some of the current properties of the lens, for instance, part of the chromatic compensation. The energy efficiency of the lens for wavelengths other than  $\lambda_0$  is markedly asymmetric. In particular, the energy efficiency for the blue light concentrates on the intermediate focus and is negligible in the distance focus. The opposite effect occurs with the red light: its energy efficiency in the intermediate focus is very low. These effects must be taken into consideration when assessing LCA compensation. Their impact on color image quality must be further investigated.

## Funding

Spanish Ministerio de Economía y Competitividad y Fondos FEDER (DPI2016-76019-R).

**Acknowledgements**

To Franco Rigato from INDO Horizons for assistance with the confocal microscope and Rosalba García Millán for assistance in the mathematical fit of experimental data.

**Disclosures**

The authors declare that there are no conflicts of interest related to this article.